A HYBRID PHOTOVOLTAIC SIMULATOR FOR UTILITY INTERACTIVE STUDIES

G. Vachtsevanos, Member, IEEE
School of Electrical Engineering
Georgia Institute of Technology
Atlanta, Georgia 30332-0250

K. Kalaitzakis
Technical University of Crete
Chania, Greece

ABSTRACT

An analog-digital photovoltaic (PV) array simulator is considered. The analog section is designed on the basis of an equivalent solar cell model while the digital section is constructed realizing the mathematical representation of the array. Fast time responses achieved by the analog section make this part suitable for the study of transient phenomena associated with the interconnected operation of PVs and the utility grid. Its digital counterpart is more appropriate for long-term experimental investigations due to its inherent accuracy and reliability. The combined hybrid simulator offers a versatile and flexible piece of apparatus capable of simulating the performance of any PV array under a variety of operating conditions. The device can be constructed with low-cost components in a compact arrangement offering transportability and ease of operation. Experimental results derived from a laboratory constructed prototype match closely the theoretically computed characteristics.

INTRODUCTION

Over the past decade, we have witnessed an increased interest in exploiting renewable energy sources, such as solar energy, for the production of electric power. Photovoltaic arrays offer an attractive means for the direct conversion of solar energy to electrical form. An intensive R&D activity has been directed, therefore, towards the development of efficient, reliable, and cost-effective photovoltaic cells as well as the design of interface and balance-of-system devices which are required for the distribution, storage, and consumption of the electric power, such as converters, inverters, maximum power trackers, batteries, etc. [1].

At an early stage of the PV development program, it was recognized that, in addition to stand-alone applications, probably the most attractive long-term utilization of PV arrays is their operation in a utility interactive mode. Although institutional and economic considerations favor such an interactive operation, many technical issues must be resolved before PVs become a viable and acceptable alternative to utility generation practices. Research problems that are currently being addressed include protection and safety issues, power quality, harmonic current generation and propagation, islanding of distributed sources, control, etc. [2,3]. It is important, therefore, to devise experimental facilities and procedures which are more compact, cost-effective, and flexible than actual array configurations for testing purposes. Moreover, environmental conditions, such as solar radiation and temperature, affect strongly the performance of PV systems; testing in a natural environment presents difficulties in achieving a full range of these environmental parameters. A PV simulator, capable of reproducing the characteristics of an actual array, while providing the flexibility of significant parameter variations, would offer a viable alternative solution to this dilemma.

In this direction, several attempts have been reported in the literature addressing the design of physical PV array simulators [4-6]. Yet, these attempts fail to provide a complete solution to the problem. In Reference 4, an analog PV simulator design is proposed. Here, adjustment of parameters, such as solar radiation, ambient temperature, and wind speed, is accomplished indirectly or may not be at all feasible. In [5], a DC rotating machine is used as the primary device in the simulator configuration, rendering the proposed equipment unacceptable for the study of transient phenomena due to the large time constants involved [7]. In general, existing devices are not capable of responding satisfactorily to both transient and steady-state requirements usually imposed on actual PV arrays under utility interactive operation.

This paper is concerned with the design of a hybrid (analog-digital) PV array simulator which capitalizes upon the unique advantages of analog and digital techniques. Thus, the fast time response of the analog section permits the study of transient phenomena, while the digital section of the simulator provides the accuracy, stability, and reliability required for the simulation of quasi steady-state conditions, and the flexibility necessary for the adjustment of external parameters.

THE SIMULATOR CONFIGURATION

Consider the block-diagrammatic configuration shown in Figure 1. The principle characteristic of this approach is the common power supply, shared by both sections, with a resultant reduction in cost and size of the facility. The analog and digital sections

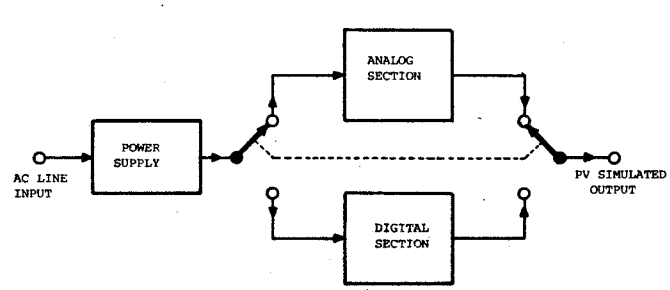

Figure 1. Block Diagram of the Two Sections of the PV Array Simulator.

of the simulator are clearly distinguished and the figure also illustrates the switching arrangement required to select one or the other mode of operation. The input to the power supply is fed from an AC source.

86 SM 465-9 A paper recommended and approved by the IEEE Power Generation Committee of the IEEE Power Engineering Society for presentation at the IEEE/PES 1986 Summer Meeting, Mexico City, Mexico, July 20 - 25, 1986. Manuscript submitted January 30, 1986; made available for printing April 25, 1986.

Printed in the U.S.A.

At the simulator output, any load or interface device may be connected as long as the load requirement is within the nominal simulator power capacity. The main simulator characteristics depend upon the device's operating state and are as follows:

A. Analog Section

The fast response of the analog section makes it ideally suitable for the study of an interconnected system's transient behavior. A line or self-commutated inverter may be connected directly to its output and both the input current and voltage waveforms recorded. Because of the high power requirements of the analog section, its utility is limited to test studies which may be completed in short periods of time and which seek the system's short-term transient behavior.

B. Digital Section

The low power consumption of the simulator, when operating at its digital mode, permits its utility for long-term measurements. Moreover, the use of a microprocessor-based controller, in this same section, provides the following additional capabilities:

1. It is possible to simulate any PV array, as long as its characteristics are known [8].
2. The simulator characteristics match those of the actual array accurately.
3. The microprocessor may be programmed to simulate different real PV array conditions including variations in temperature, cloud cover, etc. [7].

This section is not suitable for studies that involve the transient behavior of the PV array and load.

A detailed description of each simulator section follows and performance characteristics are illustrated via the design of a PV simulator with a rated power capacity of 2 kW. The design approach may be easily extended to arrays of different characteristics and power ratings. The power supply remains essentially the same having a minimum impact on the design process. Two points must be considered: (1) the voltage level at the output of the supply must be greater than the open-circuit voltage of the array to be simulated; and (2) the power supply current must be at least equal to $n_p I_{LG}$, where n_p is the number of cell branches connected in parallel and I_{LG} the light generated cell current, so that the simulator operating characteristics may extend throughout the useful array v-i region.

THE ANALOG SECTION

Design of the simulator's analog section is based upon a physical representation of the equivalent circuit of a photovoltaic cell, which constitutes the basic building block of the array. A widely accepted form of the cell's equivalent circuit is shown in Figure 2 [9]. The current source I_{LG} represents the light generated cell current and is a function of the cell characteristics, its temperature, and the solar radiation. A diode is used to represent the silicon P-N junction, R_{sh} is the parallel resistance, R_s the series resistance and, finally, C the combined junction and diffusion capacitance [10].

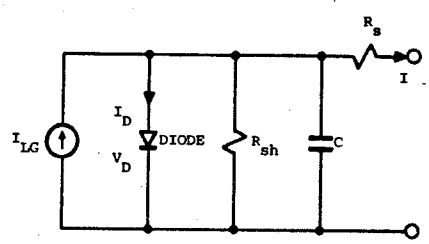

Figure 2. The Equivalent Model of the Solar Cell.

A PV array consists of the series and parallel connection of cells. Suppose that n_s identical cells are connected in series to form a branch and n_p branches are connected in parallel to form the array. Figure 3 depicts the equivalent circuit of the total series-parallel configuration. The light generated current source, in this case, is equal to $n_p I_{LG}$, while

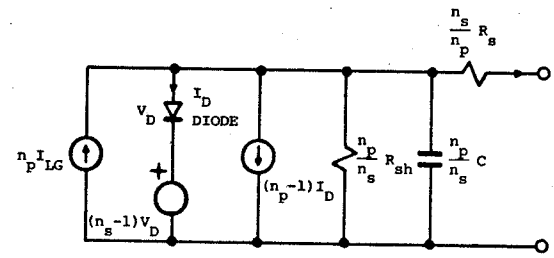

Figure 3. The Equivalent Model of a PV Array with n_s x n_p Cells.

the diode remains the same as in the single cell situation with operating characteristics V_D and I_D. The dependent voltage source $(n_s-1)V_D$ represents the voltage drop across the remaining n_s-1 diodes connected in series; the total branch voltage drop is thus $n_s V_D$. The dependent current source $(n_p-1)I_D$ stands for the current through the remaining n_p-1 parallel cell branches, so that the sum of this current and that of the n_pth branch is equal to $n_p I_D$. Values for the series and parallel resistances and for the array capacitance are easily computed.

The design of the array's analog section is based upon the equivalent circuit of Figure 3. A block diagram of the proposed scheme is depicted in Figure 4. The input of the unit is supplied from a DC voltage source. Control element No. 1, in series with a current limiter and the supply source, forms a current

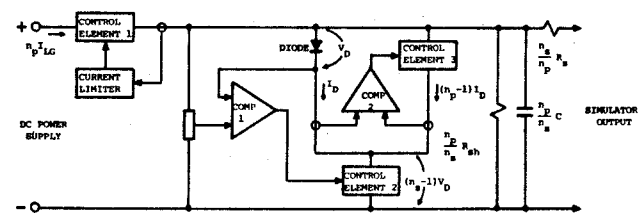

Figure 4. Block Diagram of the Analog Section.

generator which is regulated to provide an amount of current equal to $n_p I_{LG}$. The diode is the element which mainly simulates the v-i characteristics of the PV array. Let V_D the voltage across and I_D the current through the diode. Comparator No. 1 compares the diode voltage V_D with a fraction of the unit's output voltage and adjusts control element No. 2 so that a voltage of $(n_s-1)V_D$ volts is developed across it. The total output voltage becomes, therefore, equal to $n_s V_D$. Comparator No. 2 compares the diode current I_D with a fraction of the current through the parallel branch and adjusts control element No. 3 so that the parallel branch current is equal to $(n_p-1)I_D$. Thus, the total current of the branches is $n_p I_D$. The remaining elements (two resistors and a capacitor), with their

values shown in Figure 4, simulate the parallel resistance and capacitance and the array series resistance. From a design point of view, it is noted that control elements No. 1 and No. 2 dissipate most of the unit's power demand and, therefore, require appropriate heat removal apparatus.

The response time of the analog electronic circuitry is much faster than either the response time of the PV array or the time constant associated with the array output capacitance. Use, therefore, of the simulator for the study of transient phenomena does not present any major difficulties.

The junction and diffusion capacitance of the PV array is a function of the current I_D flowing through each PV cell and its value is, therefore, continuously varying. For this reason, a capacitor with a value of $\frac{n_p}{n_s} C$ is connected at the output of the analog section, as shown in Figure 4. The capacitance C may be computed through the relations [10]:

$$C = C_D + C_j \tag{1}$$

$$C_D = k_{DL} \frac{I_{LG} - i_s/n_p}{T} \tag{2}$$

$$C_j = k_j (k_T T + v_s/n_s)^{-1/2} \tag{3}$$

where k_{DL}, k_j, and k_T are constants whose values depend upon the array characteristics. Relations (2) and (3), for a typical array configuration, may be approximated by

$$C_D \approx 11838 \frac{I_{LG} - i_s/n_p}{T} \ (\mu F) \tag{4}$$

$$C_j \approx 1.3 \ \mu F \tag{5}$$

The remaining quantities appearing in (1)-(5) are defined in the following paragraph. At the diode position, an appropriate semiconductor device is placed whose behavior approximates, as closely as possible, the PV array characteristics. The actual diode selection is carried out experimentally.

THE DIGITAL SECTION

Design of the simulator's digital section is based on a realization of the array mathematical model. The equations describing the operation of a PV array are written as [11]:

$$i_s(v_s) = n_p I_{LG} - n_p I_{os} \left(e^{Gv_s/n_s} - 1\right) \tag{6}$$

$$G = \frac{1}{AT_c k/q} \tag{7}$$

$$I_{os} = I_{or} \left[\frac{T_c}{T_r}\right]^3 e^{\frac{E_{Go}}{Bk/q}\left[\frac{1}{T_r} - \frac{1}{T}\right]} \tag{8}$$

$$I_{LG} = \left[I_{SCR} + k_I (T_c - 301.18)\right] \frac{H}{100} \tag{9}$$

where:

i_s = PV array output current
v_s = PV array output voltage
n_s = number of cells connected in series
n_p = number of cell branches connected in parallel
I_{LG} = light generated current
I_{or} = reverse saturation current at T_r (= 19.9693 x 10^{-6}A)
A = B = ideality factors (= 1.92)
k = Boltzmann's constant
q = electronic charge
T_r = reference temperature (= 301.18°K)
I_{os} = cell reverse saturation current
T_c = cell temperature in °C
T = cell temperature in °K
k_I = short-circuit current temperature coefficient at I_{SCR} (= 0.0017 A/°C)
H = cell illumination (mW/cm^2)
I_{SCR} = cell short-circuit current at 28°C and 100 mW/cm^2 (= 2.52 A)
E_{Go} = band gap for silicon (= 1.11 eV)
R_s = series resistance (neglected)
R_{sh} = shunt resistance (neglected).

The array temperature, T_c, is given, approximately, by the relation [8,12]:

$$T_c = 3.12 + 0.25 H + 0.899 T_a - 1.3 w_s \tag{10}$$

where:

T_a = ambient temperature in °C
w_s = wind speed in m/sec.

The characteristics of any PV array may be simulated through Equations (6)-(10) under a variety of operating conditions (temperature variations, wind speed variations, cloud cover, etc.). These relations, together with the corresponding subroutines controlling the operation of the A/D and D/A converters, form the microprocessor program. The microprocessor controls the remaining electronic circuitry, as shown in Figure 5. A description of the operation of the circuit depicted in Figure 5 follows.

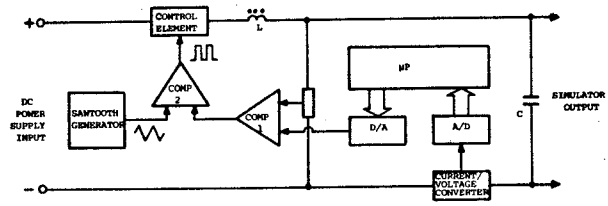

Figure 5. Block Diagram of the Digital Section.

A current-to-voltage converter unit monitors the simulator's output current and produces a proportional voltage level. This signal, through an A/D converter, is fed to the microprocessor. The program estimates the output voltage of the simulator, corresponding to the measured current, for a given PV array. This voltage is converted to analog form through a D/A converter. The rest of the circuitry is designed to develop a voltage at the simulator output terminals equal to the computed value. The components comparator No. 1, comparator No. 2, sawtooth generator, and the control element form a classical switching regulator unit. Comparator No. 1 compares the output voltage with the signal originating from the D/A converter. Next, with assistance from the sawtooth generator and comparator No. 2, feeds to the element pulses of an appropriate duration. Thus, the control element allows for current pulses to be transferred through. These pulses are finally smoothed by the inductance L and capacitance C so that, at the simulator's output terminals, the DC voltage computed by the microprocessor appears.

The procedure outlined above is continuously repeated regardless of whether the load is changing or remains constant. The circuit monitors, therefore, constantly any load variations.

Because of the computation time involved, the time required for A/D and D/A conversions, and the LC time constant, it is not possible to track accurately certain loads, such as an inverter operating at a frequency of 50 or 60 Hz. Since, though, in practical applications of PV arrays connected to a load through a voltage-fed inverter, a large capacitor (of the order of 10,000 μF) is inserted between the array and the inverter to smooth out the current waveform, utility of the digital section of the simulator becomes feasible in this situation without introducing significant errors.

The parameters n_s, n_p, H, T_a, and w_s are program input variables. Data associated with cell fabrication features are internal to the program.

The use of a switching mode to regulate the output voltage results in a substantial reduction of the power consumed by the simulator. Thus, two important economic features of the proposed digital design refer to the utility of low-cost components and the energy savings achieved for long-term experimental testing procedures.

RESULTS

A. Analog Section Performance

In order to verify the feasibility of the proposed analog section design, a 2 kW array was used with a current-voltage characteristic curve as shown in Figure 6. The analog section was adjusted and simulated results were recorded as shown in the same figure (dashed line). The difference between the actual and the simulated curves is small and rather insignificant

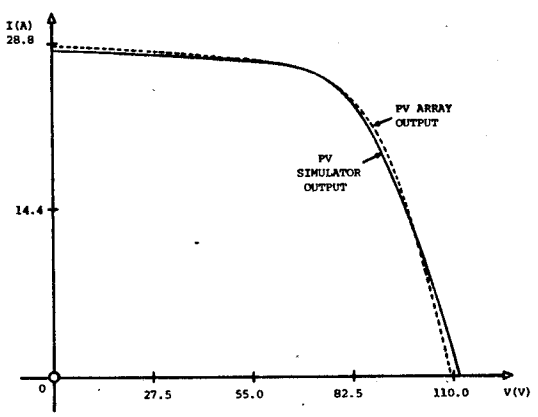

Figure 6. Comparison Between Measured and Simulated Array Characteristics.

when the simulator is used to study the transient behavior of a PV system. The equivalent output capacitance of the analog section, without the $\frac{n_p}{n_s}$ C element was measured to be 0.07 μF. This value is negligible compared to the corresponding array capacitance. The latter is calculated from Equations (4) and (5) and is approximately equal to $\frac{n_p}{n_s}$ C = 0.57 μF. The analog section design is, therefore, complemented with a capacitor of 0.5 μF at the section's output terminals so that the simulator's behavior matches accurately the transient response of an actual PV array.

B. Digital Section Performance

An experimental verification of the digital section was conducted using a series of static loads and simulating the same 2 kW PV array as in the analog case. Figure 7(a) shows the computed and the measured v-i characteristic curves for the actual array and the

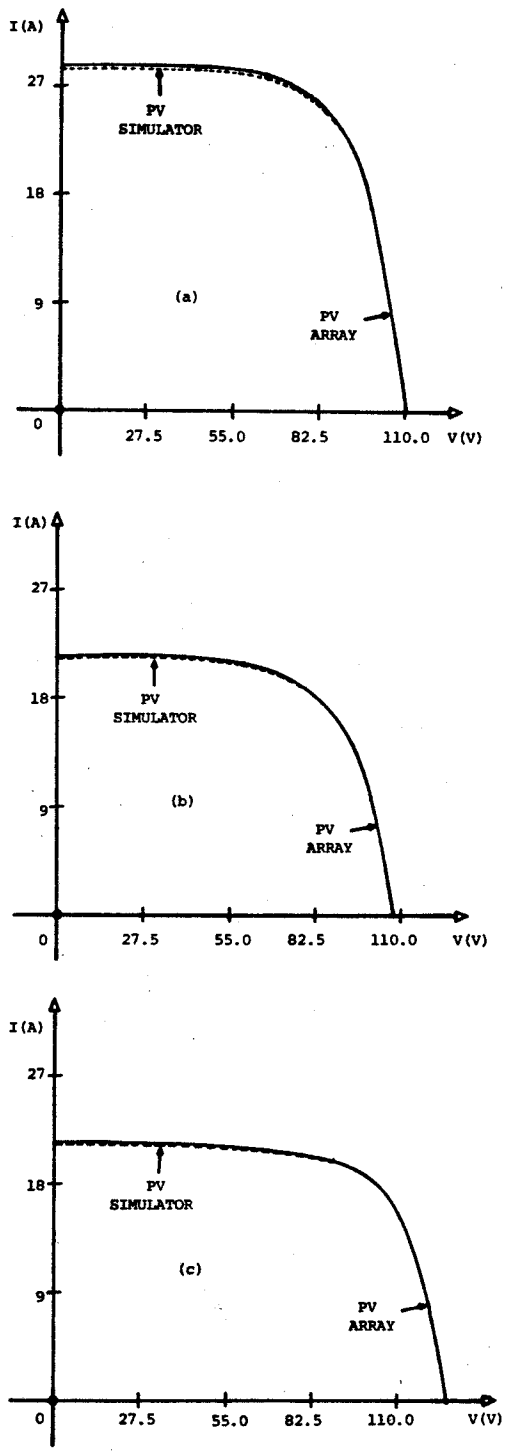

Figure 7(a), (b), and (c). Comparison Between Measured and Simulated Array Characteristics for Various Operating Conditions.

simulator, respectively. Parameter values used for the simulation are n_s = 220, n_p = 18, H = 100 mW/cm^2, and T_c = 64°C. Deviations from the theoretical PV array behavior are observed to be negligible.

Figures 7(b) and (c) depict similar comparisons. Parameter values for Figure 7(b) are: n_s = 220, n_p = 18, H = 75 mW/cm^2, T_c = 64°C. For 7(c), the parameter values were chosen to be: n_s = 220, n_p = 18, H = 100 mW/cm^2, and T_c = 28°C. In both these last figures the lack of any significant discrepancies between computed and experimental results is evident.

CONCLUSIONS

The integrated design of an analog-digital simulator permits the physical simulation of any PV array under a wide range of operating conditions. The analog section provides for a fast operating response making it suitable for studies which are intended to test the transient behavior of a PV system. The digital section, on the other hand, offers the unique advantages of a cost-effective implementation, accuracy and ease of simulation, as well as flexibility in incorporating changes of such environmental parameters as solar radiation, temperature, etc.

The simulator can be used for a variety of studies involving the interconnected operation of PVs with the utility grid. It provides the versatility and cost-effectiveness required for a diverse grouping of experiments which may impose different time and parameter constraints. Thus, the same apparatus may be employed to study harmonic injection phenomena, as well as islanding and surge protection conditions.

REFERENCES

1. S. Krauthamer, et al., "Photovoltaic Power Conditioning Subsystem: State of the Art and Development Opportunities," DOE/ET-20356-9, Jan. 1984.

2. Systems Control, Inc. and J.B. Patton, "Interconnecting DC Energy Systems: Responses to Technical Issues," EPRI AP/EM-3124, June 1983.

3. M. Kuliasha and T. Reddoch, "Research Needs for the Effective Integration of New Technologies into the Electric Utility," Proc. of Conference sponsored by DOE, CONF-820772, May 1983.

4. D.R. Smith, G.A. O'Sullivan, and F.K. O'Sullivan, "The Design and Performance of an 11 kW Solar Array Simulator," PESC '80 Record, pp. 220-225, June 1980.

5. M.A. Slonim, E.K. Stanek, and A. Imeche, "Analysis of Inverter Models and Harmonic Propagation, Part I: A Physical Simulator for Large Solar Cell Arrays," Contractor Report, Sandia National Laboratories, SAND83-7040/1 of 3, pp. 1-112, Sept. 1984.

6. G.J. Vachtsevanos and G.J. Grimbas, "A Photovoltaic Simulator," International Journal of Solar Energy, Vol. 1, No. 4, pp. 285-292, 1983.

7. D.P. Caroll, et al., "Dynamic Simulation of Dispersed Grid Connected Photovoltaic Power Systems: Task 1 - Modeling and Control," Contractor Report, Sandia National Laboratories, SAND83-7018, pp. 1-118, Nov. 1983.

8. V.V. Risser and M.K. Fuentes, "Linear Regression Analysis of Flat-Plate Photovoltaic System Performance Data," Proc. of Fifth E.C. Photovoltaic Solar Energy Conference, pp. 623-627, 1983.

9. D.L. Evans, W.A. Facinelli, and L.P. Koehler, "Simulation and Simplified Design Studies of Photovoltaic Systems," Contractor Report, Sandia National Laboratories, SAND80-7013, 1980.

10. D. Zerbel, "AC Impedance of Silicon Solar Cells," Intersociety Energy Conversion Engineering Conf., Vol. 1, pp. 10-15 to 10-18, 1970.

11. R.L. Steigerwald, A. Ferraro, and R.E. Tompkins, "Investigation of a Family of Power Conditioners Integrated into the Utility Grid. Category 1 - Residential Power Conditioner Final Report," Contractor Report, Sandia National Laboratories, SAND81-7031, pp. 1-94, Sept. 1981.

12. W.R. Anis, R.P. Mertens, and R.J. Overstraeten, "Calculation of Solar Cell Operating Temperature in a Flat Plate PV Array," Proc. of Fifth E.C. Photovoltaic Solar Energy Conf., pp. 520-524, 1983.